Dietary Cocos nucifera milk mitigates D-galctose-induced aging and neurotoxicity in Drosophila melanogastervia modulation of oxidative stress and neurotransmitter dysfunction

Muideen Tunde Arogundade

muideen.arogundade@pgc.uniosun.edu.ng

Department of Biochemistry, College of Science, Engineering and Technology, Osun State University, Osogbo, Nigeria https://orcid.org/0009-0001-9699-7954

Rafiu Adekunle Raji

Department of Biochemistry, Federal University of Agriculture and Developmental Studies, Iragbiji, Nigeria

Kamiludeen Ayinla Jimoh

Department of Biochemistry, Faculty of Sciences, University of Ilesa, Ilesa, Nigeria

Tope Atere Gafar

Department of Medical Biochemistry, College of Health Science, Osun State University, Osogbo, Nigeria

Research Article

Keywords: Coconut milk, Aging, D-galactose, In silico, Drosophila melanogaster, Neurodegenerative disorder

Posted Date: July 3rd, 2026

DOI: https://doi.org/10.21203/rs.3.rs-10221726/v1

Additional Declarations: The authors declare no competing interests.

Dietary *Cocos nucifera* milk mitigates D-galctose-induced aging and neurotoxicity in *Drosophila melanogaster* via modulation of oxidative stress and neurotransmitter dysfunction

Muideen Tunde Arogundade[1*], Rafiu Adekunle Raji[2], Kamiludeen Ayinla Jimoh[3], Tope Atere Gafar[4]

[1]Department of Biochemistry, College of Science, Engineering and Technology, Osun State University, Osogbo, Nigeria.

[2]Department of Biochemistry, Federal University of Agriculture and Developmental Studies, Iragbiji, Nigeria.

[3]Department of Biochemistry, Faculty of Sciences, University of Ilesa, Ilesa, Nigeria.

[4]Department of Medical Biochemistry, College of Health Science, Osun State University, Osogbo, Nigeria.

*Corresponding author: muideen.arogundade@pgc.uniosun.edu.ng

[2] rafiu.raji@fuadsi.edu.ng

[3] kamiludeen_jimoh@unilesa.edu.ng

[4] tope.atere@uniosun.edu.ng

Abstract

Background The prevalence of aging and age-related neurodegenerative diseases is a global concern. The impact of coconut milk (CM) as an anti-aging and neuroprotective agent is yet to be fully understood, despite its nutritional importance.

Objective This study aimed to examine the neuroprotective and anti-aging potential of CM against D-galactose-induced aging using the *Drosophila melanogaster* (*D. melanogaster*) mode.

Methods Flies aged three to five days were separated into four groups, with five replicates each (n = 50). Group 1 received an untreated diet, group 2 received 25 mg of D-galactose (D-gal) in their diet, group 3 received 2.5 ml/g of diet, and group 4 received the combination of 25 mg of D-gal and 2.5 ml/g of CM diet. The inducement lasted for 14 days. Afterward, behavioral and biochemical tests were conducted. The bioactive compounds in CM were identified by gas chromatography-mass spectrometry (GC-MS) analysis, and the main bioactive components were docked into the binding pockets of glutathione-s-transferase-2 (GST-2) and acetylcholinesterase (AChE).

Results CM significantly mitigated the lifespan, locomotion, and eclosion rate alterations induced by D-gal and also attenuated the redox status and neurotransmitter disruptions. Also, oleic acid, one of the bioactive components in CM, presented with the highest binding affinities of -7.7 kcal/mol and -5.1 kcal/mol when docked against AChE and GST-2, respectively.

Conclusion The behavioral, biochemical, and in silico results obtained give credence to the fact that CM possesses ameliorative potential against age-related locomotive dysfunction, reproductive decline, and neurodegenerative disorders, possibly via its antioxidant and neuromodulatory properties.

Keywords Coconut milk, Aging, D-galactose, *In silico*, *Drosophila melanogaster*, Neurodegenerative disorder

Graphic Abstract

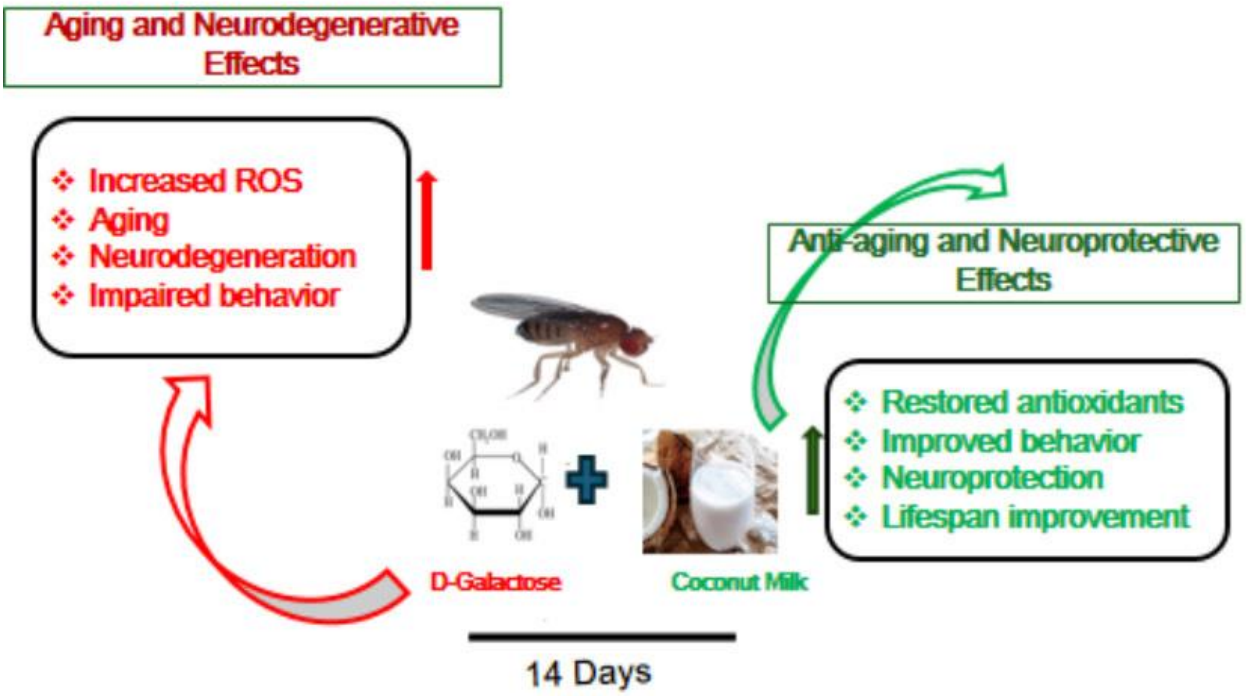

1. Background

Aging is an intricate process and a risk factor for the emergence and progression of many illnesses [1]. The biological process of aging is characterized by a gradual deterioration in cellular and organismal activities [2], which also results in a consistent and irreversible decline in physical function [3], DNA damage, NAD^+ loss, telomere dysregulation, stem cell fatigue, mitochondrial dysregulation, and autophagy disorders are only a few of the major causes of aging [4]. These aging hallmarks are connected, however, the underlying causes are inflammation and free radical-induced oxidation which brought about a new theory of aging called the "oxy-inflamm-aging theory"[5]. Particularly, neurodegenerative disorders are the common age-related disorders [6] Neurons are most vulnerable to aging [7] and are usually accompanied by increased numbers of senescent cells in the brain, central nervous system atrophy, and protein aggregation [8].

Several foods, including cherries, plums, yogurt, honey, and butter, contain D-galactose (D-gal), which galactokinase and uridyltransferase convert to glucose at normal levels [9-10]. However, when D-gal is administered over an extended period of time, the body shifts into unwanted metabolic pathways [11]. D-gal forms advanced glycation end products (AGEs) by its reaction with free amines and amino acids [12]. Similarly, galactose oxidase catalyzes the conversion of D-gal into hydrogen peroxide at high concentrations, which is also converted by aldose reductase to galactitol without being subsequently broken down and is instead stored in cells, resulting in the buildup of free radicals that might upset the normal osmotic pressure and redox balance [13]. Overall, chronic administration of D-gal to mice, rats, and *Drosophila melanogaster* (*D. melanogaster*) has been shown to accelerate senescence and cause symptoms that resemble natural aging, including decreased antioxidant enzyme capacity, shortened lifespan, mitochondrial dysfunction, and insensitive immune response [14]. Mahdi *et al*. narrated that mouse models

exposed to D-gal developed neurotoxicity, such as cognitive and behavioral deficits [15]. D-gal is a frequently used experimental aging and neurodegeneration inducer [4, 16] due to short study duration, convenience of use, low cost, and lower risk of animal death in in vivo models [17].

The development of novel anti-aging medications continues to be a key priority to delay and have a healthy aging process [18]. Nutrition therapy (NT) has emerged as an important area of interest for those seeking better health, especially with regard to aging [19-21]. Preclinical research provides compelling evidence that a range of dietary factors, including calorie intake, carbohydrates, protein, and fat content, are paramount for controlling aging processes, longevity, and the emergence of age-related diseases like dementia [22-23]. One of the most well-known and commonly used palm trees that produces coconut fruit is the "tree of life," *Cocos nucifera* [24]. Given its high fat content, coconut milk (CM), the liquid extract made from coconut fruit, has a high calorie density. However, its lipid profile is unique because the bulk of its fat is made up of medium-chain triglycerides (MCTs) [25], which directly enhanced mitochondrial biosynthesis, triggered the production of albumin, and improved physical function [26].

Additionally, Russo *et al*. stated that CM contains polyphenols that can alter several aging-associated factors [27]. When compared to cow's and goat's milk, it contains the highest amounts of antioxidant activity [28]. Unlike coconut oil and water, CM contains a broader range of bioactive constituents, including lipids, phenolic antioxidants, and micronutrients [29], which may enhance its neuroprotective and anti-aging potential. With all these, the anti-aging and neuroprotective potential of CM remains unexplored. Due to its short lifetime and life cycle, high number of progeny per adult, low cost, and ease of handling and maintenance [30] and also expressing about 77% of genes linked to age-related disorders in humans [31], *Drosophila* is a perfect model organism to investigate mechanisms of aging and longevity. So, we examined the

anti-aging and neuroprotective effects of CM using the D-gal-induced *Drosophila* aging model. Also, gas chromatography–mass spectrometry (GC-MS) was utilized to detect the phytochemicals that are present in CM and the bioactive compounds were docked with key enzymes related to neurodegeneration. This study hypothesizes that CM will attenuate age-like phenotypes by restoring redox status, ameliorating lipid peroxidation, and suppressing neurodegeneration in the D-gal-induced aging *D. melanogaster* model.

2.0 Material and method

2.1 Chemicals

The coconut fruits were acquired from Oke Baale market in Osogbo, Osun State, Nigeria, while agar-agar, nipagin, yeast, ethanol, maize meal, and D-gal (99% purity) were purchased from Nanjing Jiancheng Biochemical Co., Ltd. (Shanghai, China). In every other case, analytical-grade chemicals and reagents were used.

2.2 Preparation of coconut milk

To produce the CM, Dr. G.O. Okunola of Osun State University's Plant Biology Department in Osun State, Nigeria, verified the authenticity of the *Cocos nucifera* fruit samples. After cracking open the *Cocos nucifera* fruits to reveal the meat, they were cleaned with distilled water and sliced into little pieces. Then 50 g of the sliced coconut meat and 100 ml of double-distilled water were combined in an electric blender machine. Aftermath, a cotton sieve was employed to filter the ground mixture, which yielded an average of 64.2 ml CM; the remaining filtrate (CM) was utilized in the study [32]. Throughout the experiment, the extract was made fresh each day for diet preparation.

2.3 GC-MS analysis of CM

Gas chromatography coupled with mass spectrometry (GC–MS) was conducted using an Agilent 5975C Inert MSD with a Triple-Axis Detector linked to an Agilent 7890A GC system (Agilent Technologies, USA). Helium was utilized as the carrier gas, and the system had an autosampler with a 10 µL syringe.

A capillary column coated with phenyl methyl siloxane measuring 30 m in length, 0.25 µm in film thickness, and 0.25 mm in internal diameter was used to accomplish chromatographic separation. The carrier gas pressure was 16.2 psi, the electron ionization (EI) source temperature was 250°C, the temperature at the interface was 300°C, in split mode, the injection volume was 1 µL with a split ratio of 1:50. The injector's temperature was also maintained at 300°C.

The oven temperature program was ramped up to 150°C at a rate of 4°C per minute, subsequently increased to 250°C at a rate of 20°C per minute and remained there for an additional 5 minutes after beginning at 35°C and holding it there for five minutes.

The run took 47.5 minutes. The manufacturer's MS Solution software was used for data collecting and system control. To identify the chemicals, the acquired mass spectra were matched to standard spectra from the NIST Mass Spectral Library (NIST II).

2.4 Culturing *Drosophila melanogaster*

At Osun State University's NeuroTherapeutic Laboratory (NTL) in Osogbo, Nigeria, the Harwich fly strain of *D. melanogaster* was grown on a diet of 0.7 g of Nipagin, 5 g of yeast, 52 g of cornmeal, and 7 g of agar-agar. A 12-hour cycle of day and night, as well as constant temperature and humidity, were the normal circumstances [33]. The strain was obtained from the University of

Ibadan's Biochemistry Laboratory in Oyo State, Nigeria. In this study, three- to five-day-old fruit flies were used with equal sex distribution of a ratio of 1:1 for every group.

2.5 Lifespan assay for dose determination

The therapeutic dosage of CM was determined by evaluating the effect on lifespan using the approach provided by Farombi *et al*. [34]. A variety of doses were evaluated using a small number of Drosophila flies: 1 ml/g diet, 2 ml/g diet, 2.5 ml/g diet, and 5 ml/g diet of CM in order to determine whether pretreatment had an impact on fly survival during the trial. Each death that occurred each day was given a score of one, while a score of zero indicated no fatalities. Based on the information gathered from the lifespan curve, a 2.5 ml/g diet of CM was chosen for the study.

2.6 Experimental design

CM (2.5 ml/g of diet) from the lifespan assay and D-gal (25 mg/g), also based on earlier research by Oyebode *et al*. [14] were administered to 3-5-day-old flies for 14 days as outlined below:

Groups	Treatment
1	Control (distilled water)
2	D-gal (25 mg/g of diet)
3	CM (2.5 ml/g of diet)
4	D-gal (25 mg/g of diet) + CM (2.5 ml/g of diet)

Each group has 5 replicates and n=50.

2.7 Behavioral analysis

2.7.1 Longevity assay

The longevity assay described by Men *et al*. was carried out to see if CM cures the lifespan shortfall caused by D-gal. [35]. For every experiment, four groups of 3-5-day-old flies (20 flies per vial) were randomly selected with three replicates for each group. Untreated feed was given to the control group; D-gal (25 mg/g of diet) alone to group 2; CM (2.5 ml/g of diet) to group 3; and a combination of D-gal (25 mg/g of diet) and CM (2.5 ml/g of diet) to group 4. Every three days, flies were moved to a new medium. Until every fly died, its mortality was noted, and a longevity curve was calculated and computed.

2.7.2 Assay for negative geotaxis

From each group, 20 flies were put in vertical test tubes and given fifteen minutes to acclimate before being utilized in the gravitaxis assay. Once the tube was flipped, the flies were carefully affixed to its base. The performance index (PI) was determined by counting the number of flies that climbed to a height of 17.5 cm inside the tube in eight seconds. This process was repeated three times at intervals of one minute, and the results were recorded for statistical analysis [36].

2.7.3 Olfactory function assay by smell chemotaxis

Prior to the assay, a test tube measuring 20 cm in length was filled with twenty flies and allowed to acclimate for 15 minutes. A repellant compound (100 mM benzaldehyde dissolved in a 1.5% agar solution) was placed at one end of the container. After that, the flies were tapped and gently put into the repellent. In less than one minute, the number of *D. melanogaster* in the tube that was furthest from the repellant was counted. Then the average percentage of those flies was used to

compute the Repulsiveness Index (RI). Following three iterations of the test with a one-minute lag between each, data was collected for evaluation [37].

2.7.4 Eclosion assay

The vials used to raise the flies were gathered at the conclusion of the experiment, and their development, pupation, and eclosion were observed every day. The number of adult *D. melanogaster* that successfully emerged from the pupal case was used to calculate the rate of emergence. For 21 days, the number of flies that emerged from each vial was counted and recorded for analysis [38].

2.8 Biochemical test

2.8.1 Sample preparation for biochemical analysis

Following the course of treatment, flies were put to sleep using the ice method, weighed, and homogenized at pH 7.0 in 0.1 M phosphate buffer (1 mg/10 mL) prior to being centrifuged for ten minutes at -4°C at 4000 rpm in a Thermo Scientific Sorvall Micro 17R refrigerated centrifuge. After the pellets and supernatants were separated, they were stored at -20°C in labeled Eppendorf tubes and used to analyze biochemical parameters. For each of the five duplicates, each test was run twice [34].

2.8.2 Biochemical indices determination

2.8.2.1 Assessment of catalase (CAT), glutathione S-transferase (GST), superoxide dismutase (SOD) activities and glutathione (GSH) levels

Using established spectrophotometric techniques, the activities of catalase (CAT), superoxide dismutase (SOD), glutathione S-transferase (GST), and glutathione (GSH) levels were measured.

Igbodara and Akinloye modified approach, which measures the rate of hydrogen peroxide breakdown, was used to assess CAT activity. A phosphate buffer, H_2O_2, and diluted samples were used in the assay. For two minutes, the absorbance was measured every ten seconds at 240 nm. The H_2O_2 extinction coefficient (€ = 39.4 mM^{-1} cm^{-1}) was used to calculate enzyme activity, which was then represented as micromoles of H_2O_2 broken down/minute/milligram of protein [39].

The enzymatic activity of GST was measured using the technique outlined by Habig and Jakoby. 270 µL of a solution of 20 µL of 0.25 M potassium phosphate buffer, pH 7.0, 2.5 mM EDTA, 10.5 µL of distilled water, 10 µL of 25 mM 1-chloro-2,4-dinitrobenzene (CDNB), 20 µL of sample (1:5), and 25 µL of 0.1 M GSH at 25 °C made up the reaction mixture. The final solution was measured at 340 nm for five minutes, 10 seconds at a time [40].

According to Sun and Zigman, the ability of SOD to inhibit adrenaline from auto-oxidizing was used to measure its activity [41]. Carbonate buffer, epinephrine, and distilled water made up the reaction mixture. Using 4020 M^{-1} cm^{-1} as the molar extinction coefficient (€), variations in absorbance at 480 nm were measured over a 5-minute period.

The level of the reduced form of glutathione (GSH) was estimated using the procedure described by Sedlak and Lindsay. One milliliter (1.0 ml) of supernatant was mixed with Ellman's reagent (19.8 mg of 5,5-dithiobisnitrobenzoic acid (DTNB) in 100 ml of 0.1% sodium nitrate) and 3.0 ml of phosphate buffer (0.2 M, pH 8.0). Spectrophotometry was used to detect the absorbance at 412 nm [42].

2.8.2.2 Determination of hydrogen peroxide (H_2O_2), nitric oxide (NO), and malondialdehyde (MDA) levels

Using slightly modified validated spectrophotometric assays, the amounts of nitric oxide (NO), malondialdehyde (MDA), and hydrogen peroxide (H_2O_2) were measured in homogenized Drosophila samples. To prevent pigment interference, fly eyes were carefully removed prior to inspection. The ferrous oxidation–xylenol orange (FOX1) assay, as outlined by, was used to detect absorbance at 560 nm in order to quantify H_2O_2 levels [43].

According to Eleftherianos *et al*., nitric oxide (NO) levels were indirectly estimated using the Griess reaction through the detection of nitrite and nitrate derivatives. Concentrations were determined using a sodium nitrite standard curve, and absorbance was measured at 540 nm.[44] Additionally, MDA levels were measured using the thiobarbituric acid reactive substance (TBARS) method, which was adapted from Karatas *et al*. [45].

2.8.2.3 Evaluation of neurotransmitters (acetylcholine and dopamine) levels and acetylcholine esterase (AChE) activity.

Following the manufacturer's instructions, the dopamine and acetylcholine contents of pulverized fly samples were measured using the ELISA kit (Elabscience, China). The absorbance at 450 nm was measured using a Spectramax Plus 384 microplate reader.

The Ellman *et al*. method was used to measure AChE activity. For this experiment, a buffer with 0.1 M potassium phosphate, pH 7.4, 0.8 mM acetylthiocholine as the initiator, and 1 mM DTNB was utilized. For two minutes, the reaction was recorded at 412 nm every thirty seconds [39].

2.9 Data analysis

The data is shown as mean ± SEM. ANOVA, a one-way analysis of variance, was used to evaluate significant differences between the groups under different treatments. Dunnett's post-hoc test was then performed using GraphPad Prism 8.0. However, the survival data was examined using the Kaplan-Meier analysis method and the groups were compared using the log-rank test. $P < 0.05$ was chosen as the threshold for statistical significance.

2.10 *In silico* studies

2.10.1 Retrieving and preparation of phytochemical compounds (ligands)

The 2D chemical structures of the phytochemical constituents identified by GC–MS analysis of CM were obtained from the PubChem database (link: https://pubchem.ncbi.nlm.nih.gov). After retrieval, the compounds were concatenated using Open Babel. Subsequently, the DataWarrior software was used to convert the 2D structures into their corresponding 3D conformations required for molecular docking studies.

2.10.2 Retrieving and preparation of standard compounds

The standard compound used for *D. melanogaster* acetylcholinesterase (AChE) in this study was its co-crystallized ligand, an established inhibitor. The co-crystallized ligand, identified as 9-(3-iodobenzylamino)-1,2,3,4-tetrahydroacridine, was extracted from the enzyme's active site and saved in PDB format using PyMOL software. For glutathione-S-transferase-2 (GST-2), methyldopa was used as the reference standard compound.

2.10.3 Retrieving and preparation of drug targets

The drug targets selected for this study were *D. melanogaster* AChE and GST-2. The X-ray crystallographic structures of AChE (PDB ID: 6XYU) and GST-2 (PDB ID: 1M0U) were obtained from the Protein Data Bank (link: http://www.rcsb.org/).

Protein preparation was carried out using PyMOL software. During this process, water molecules and other non-essential components were removed to optimize the structures for docking analysis. The co-crystallized ligands were subsequently extracted from the active sites of the proteins to expose the binding pockets and facilitate the determination of grid coordinates while docking.

2.10.4 Molecular docking

Following the preparation of proteins (drug targets) and ligands, molecular docking was conducted according to the protocol described by George *et al*. [46] using the AutoDock Vina option integrated in the PyRx tool. Before docking, ligand structures in MOL SDF format were transformed into PDBQT format, and Open Babel integrated with PyRx was used to minimize energy using the Universal Force Field (UFF).

The AChE grid box, measuring 25 × 25 × 25 Å, was centered at coordinates 24.2548 × 62.5745 × 9.9008 along the x, y, and z axes, respectively, during docking. For GST-2, the binding site was defined by centering the grid box at 63.7496 × −10.7406 × 6.3911 along the x, y, and z axes, using the identical grid size of 25 × 25 × 25 Å.

The standard compounds were first docked into the active sites of their respective target proteins. Subsequently, the test phytochemical compounds were docked into the same binding sites using identical grid box parameters to ensure consistency in the docking procedure.

2.10.5 Validation of docking protocol

By re-docking the co-crystallized ligands into the binding sites of their corresponding target proteins, the docking procedure was verified. The resulting poses exhibited strong agreement with the experimentally determined conformations. The root-mean-square deviation (RMSD) values were determined by Discovery Studio 2025, and these values were within the acceptable limits (≤ 2.0 Å). This indicates accurate reproduction of binding orientations and confirms that AutoDock Vina in PyRx is appropriate for predicting ligand–protein interactions. Therefore, the docking methodology employed is considered reliable, and the associated binding affinity scores are valid.

2.10.6 Protein-ligand complex visualization

Following molecular docking, the docked molecules were used to generate protein–ligand complexes using PyMOL software. Subsequently, the interactions within the protein–ligand complexes were visualized and analyzed using Discovery Studio 2025.

3.0 Results

3.1 Effect of CM on lifespan and motor tests

At first, a dose-response correlation lifespan assay (Figure 1A) was examined to see how CM exposure would affect the survival of *D. melanogaster*. The groups showed a progressive median survival increment of 17, 19, 22, 26, and 30 days for the control, 1 ml/g, 2 ml/g, 2.5 ml/g, and 5 ml/g diets, respectively. A significant difference ($p < 0.05$) was found between the groups by Kaplan-Meier survival analysis followed by the log-rank (Mantel-Cox) test; however, there was no significant difference between the 2.5 ml/g diet and 5 ml/g ($p = 0.6534$) despite 5 ml/g having a higher median survival score. Based on this, 2.5 ml/g was chosen for subsequent study.

Furthermore, when compared with the D-gal-induced lifespan shortening, co-treatment with CM significantly increased the flies' longevity ($p = 0.0015$), as displayed in Figure 1B. Also, the locomotor performance (Figure 1C) significantly decreased in D-gal-treated flies in contrast to the CM-alone and control groups ($p < 0.05$). Conversely, co-treatment with CM showed a notable enhancement in the negative geotaxis in comparison with the D-gal-treated group ($p < 0.05$), demonstrating a defensive effect against locomotor dysfunction induced by D-gal.

(A) Lifespan assay

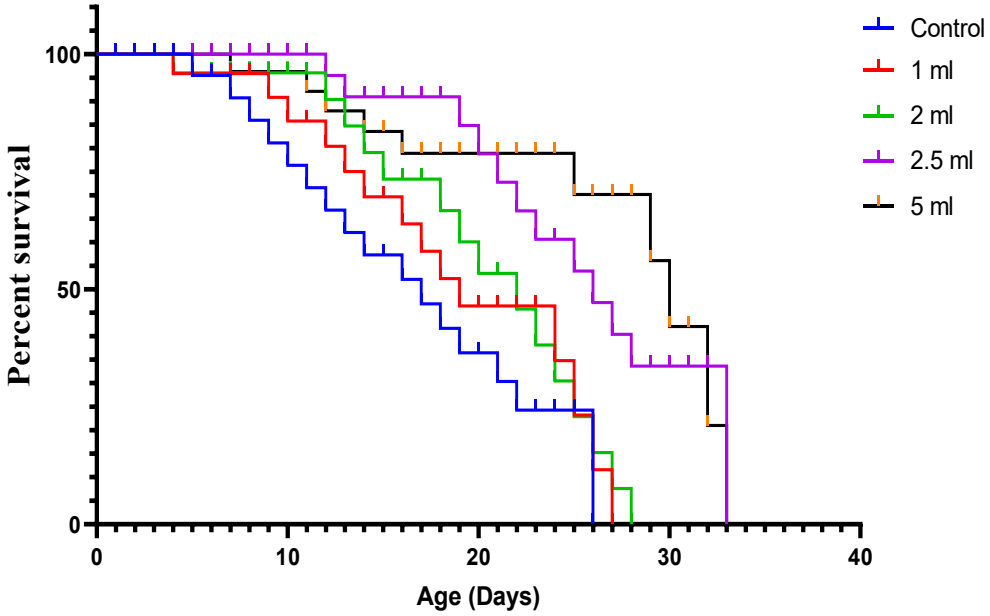

(B) Longevity assay

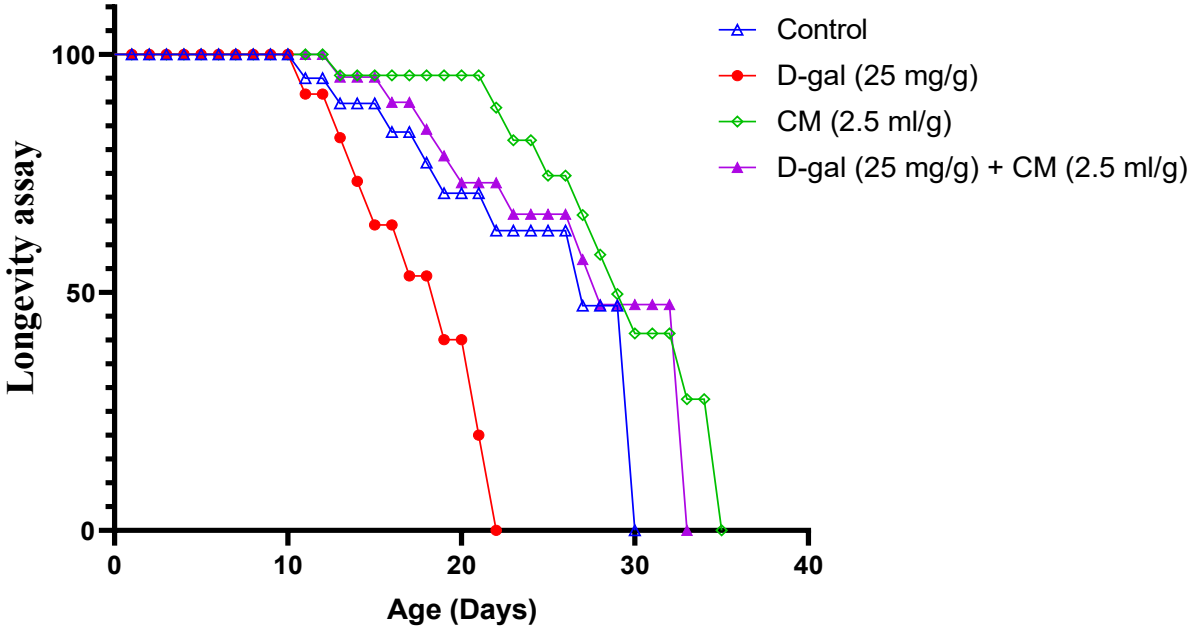

(C) Negative geotaxis

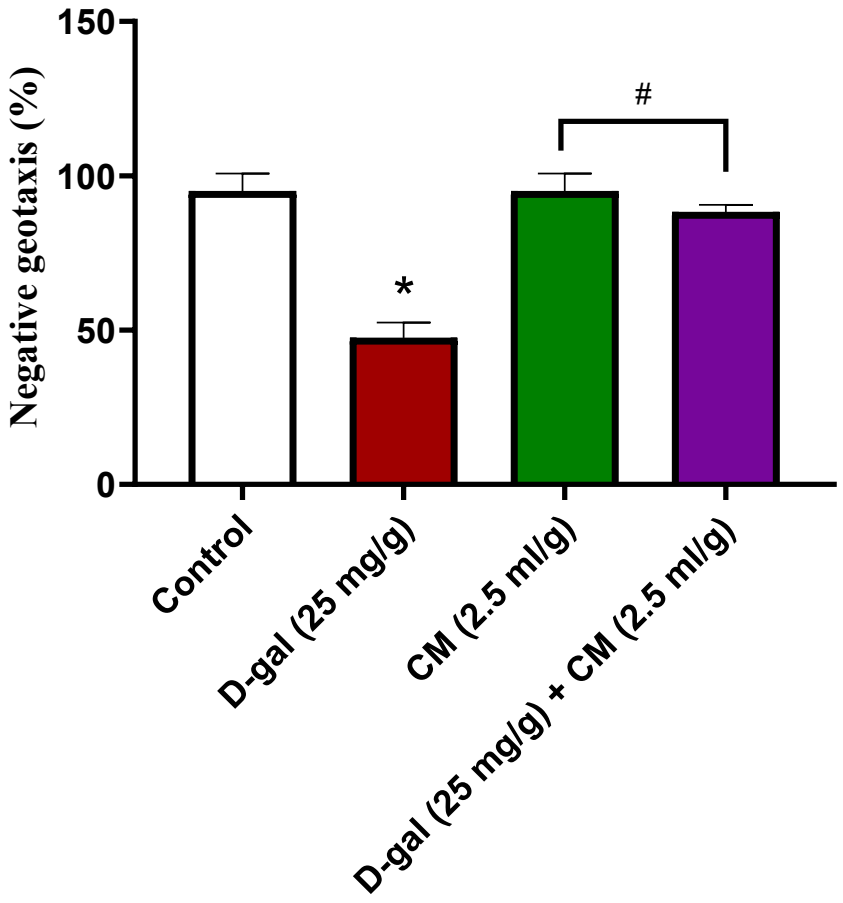

FIGURE 1: Effect of CM on lifespan and motor function in *D. melanogaster*. (A) Lifespan assay. (B) Longevity assay. (C) Negative geotaxis assay. The values are presented as mean ± SEM (n = 50). * $p < 0.05$ indicates comparison with the control group and # $p < 0.05$ indicates comparison with the D-gal group. CM denotes coconut milk (2.5 ml/g diet); D-gal represents D-galactose (25 mg/g diet).

3.2 Effect of CM on olfactory and offspring emergence assay

Figures 2A and 2B illustrate the olfactory function and eclosion rate results. In comparison to the control and CM-alone groups, D-gal-treated flies showed a significant decrease in olfactory function and eclosion rate ($p < 0.05$). On the other hand, co-treatment with CM showed a notable improvement in olfactory function and eclosion rate when compared to the D-gal-treated flies ($p < 0.05$). Nevertheless, the D-gal + CM group still showed a significant difference compared to the control group ($p < 0.05$), suggesting partial recovery of the non-motor age-related deficits.

(A) Olfactory assay **(B) Eclosion assay**

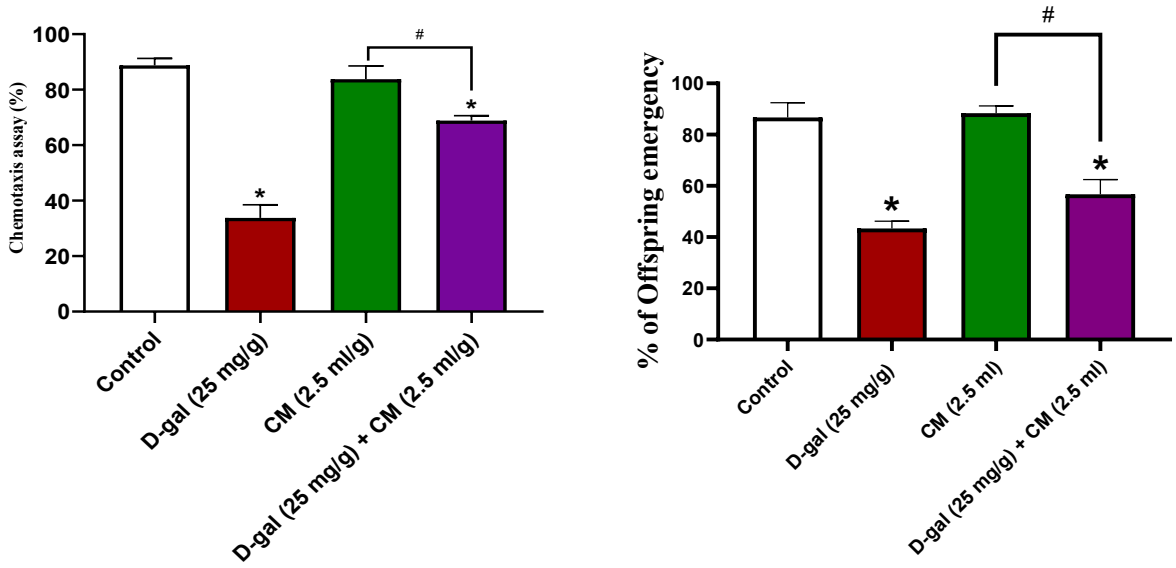

FIGURE 2: Effect of CM on olfactory function and eclosion rates**:** (A) Olfactory assay. (B) Eclosion rate. The results are presented as mean ± SEM (n = 50). The values are presented as mean ± SEM (n = 50). * $p < 0.05$ indicates comparison with the control group and # $p < 0.05$ indicates comparison with the D-gal group. CM denotes coconut milk (2.5 ml/g diet); D-gal represents D-galactose (25 mg/g diet).

3.3 Effect of CM on oxidative stress and antioxidant parameters

The control and CM-alone groups exhibited significantly lower levels of MDA (Figure 3A), H_2O_2 (Figure 3B), and NO (Figure 3C) compared to both the D-gal-treated and the D-gal + CM groups ($p < 0.05$). An exception was observed in H_2O_2 levels, where no significant difference was found between the CM-alone and the D-gal + CM group. Notably, co-treatment with CM significantly reduced all oxidative stress markers tested when compared to the D-gal-treated group ($p < 0.05$), indicating attenuation of oxidative stress.

The D-gal-treated flies exhibited significantly reduced antioxidant activity, as evidenced by reduced CAT activity (Figure 3D), SOD activity (Figure 3E), GSH levels (Figure 3F), and GST activity (Figure 3G), compared to both the control and CM-alone groups ($p < 0.05$). Additionally, CAT activity in the D-gal + CM group did not differ significantly from either the control or CM-alone groups, while GSH levels were also comparable to the control group. Furthermore, co-treatment with CM demonstrated significant improvement in all antioxidant parameters compared to the D-gal-treated group ($p < 0.05$), confirming restoration of antioxidant defenses.

(A) **MDA level**

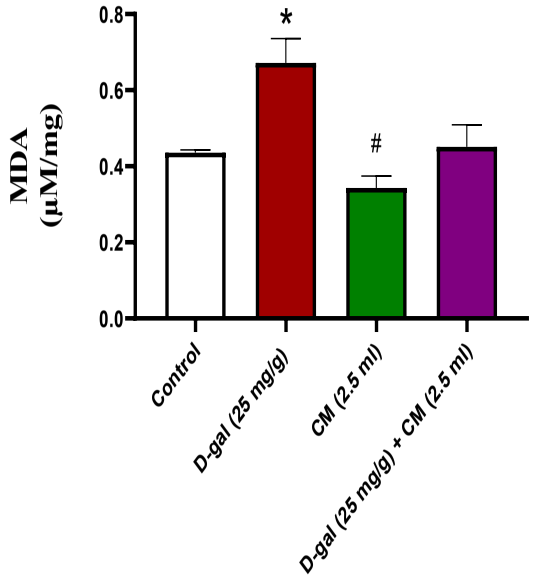

(B) **H_2O_2 level**

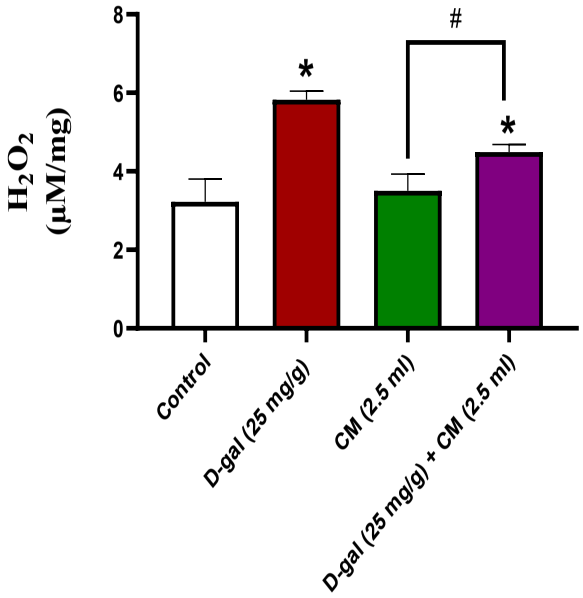

(C) **NO level**

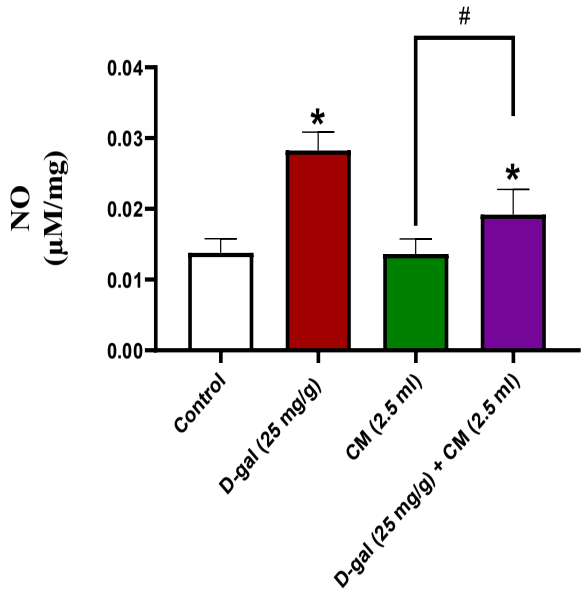

(D) **CAT activities**

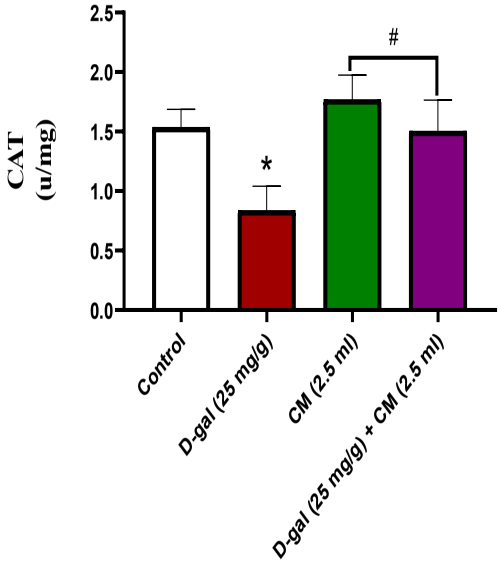

(E) SOD activities

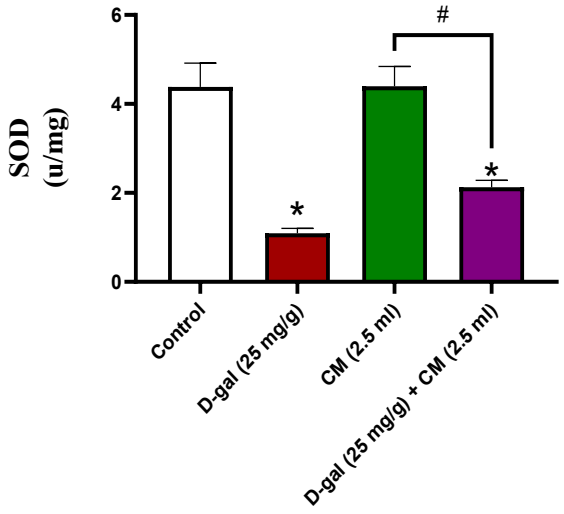

(F) GSH level

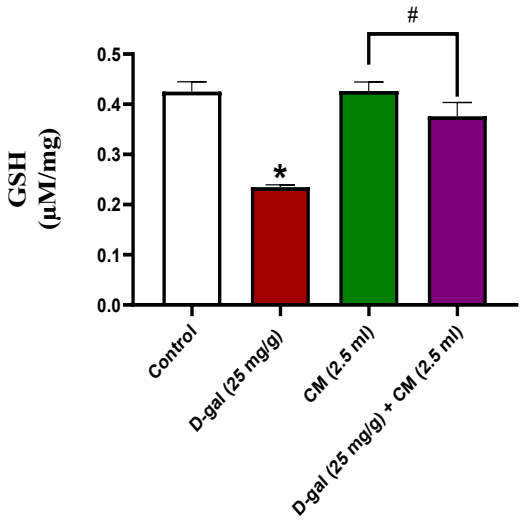

(G) GST activities

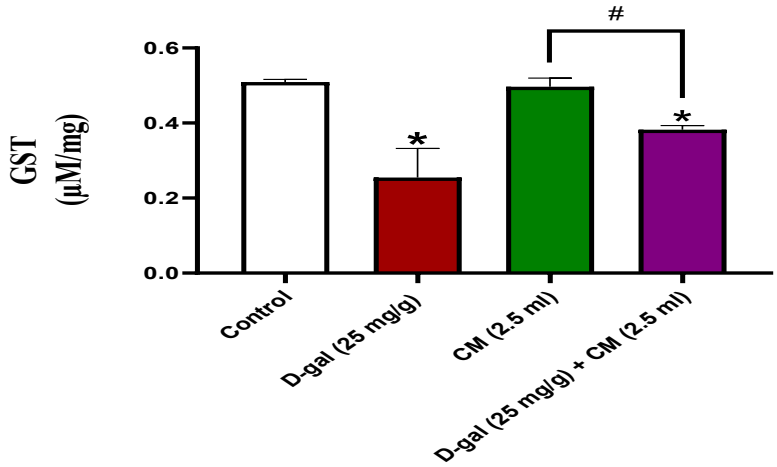

FIGURE 3: Effect of CM on Oxidative Stress Parameters (A) MDA Level (B) H_2O_2 Level (C) NO Level (D) CAT Activities. (E) SOD Activities. (F) GSH Level. (G) GST Activities**.** The values are presented as mean ± SEM (n = 50). * $p < 0.05$ indicates comparison with the control group and # $p < 0.05$ indicates comparison with the D-gal group. CM denotes coconut milk (2.5 ml/g diet); D-gal represents D-galactose (25 mg/g diet).

3.4 Effect of CM on AChE activity and neurotransmitters level

In this study, both the D-gal-treated flies and the D-gal + CM group showed a significantly lower levels of ACh (Figure 4B) and dopamine (Figure 4C) in relation to the control and CM-alone groups ($p < 0.05$). In contrast, AChE activity (Figure 4A) was significantly elevated in the D-gal-treated group in comparison with the control ($p < 0.05$). However, no significant differences in AChE activity were noted between the control and D-gal + CM groups or between the CM-alone and the D-gal + CM groups. Moreover, co-treatment with CM significantly ($p < 0.05$) reduced AChE activity and elevated ACh and dopamine levels relative to the D-gal-treated group, suggesting restoration of cholinergic and dopaminergic function.

(A) AChE activities

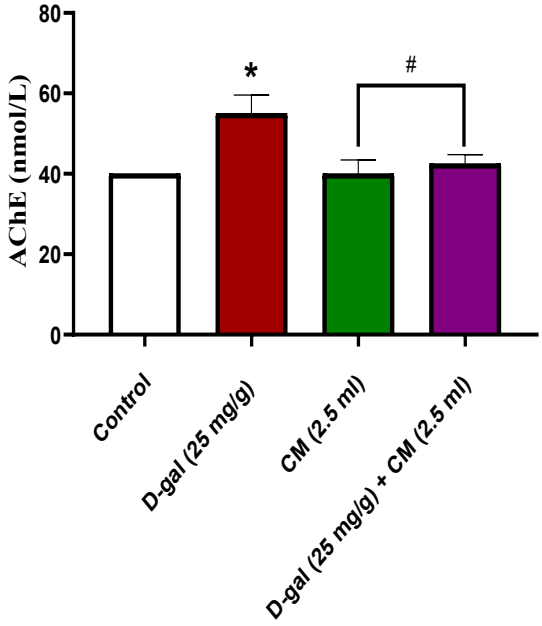

(B) ACh level

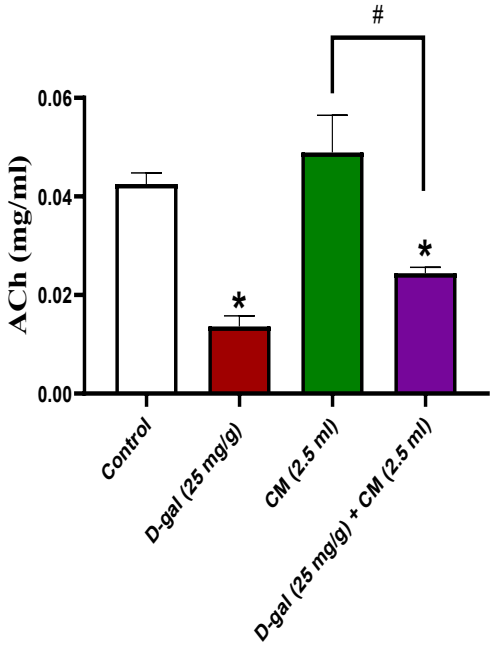

(C) Dopamine level

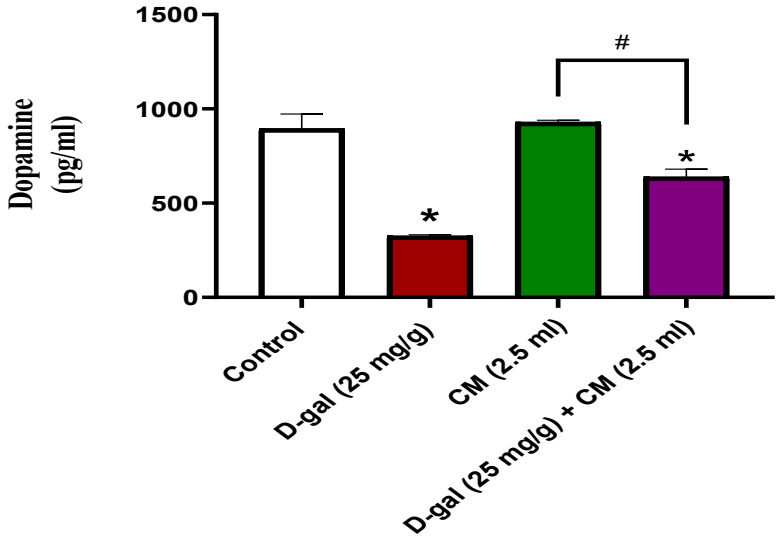

FIGURE 4: Effect of CM on Neurotransmitters (A) AChE Activities (B) ACh Level (C) Dopamine Level. The values are presented as mean ± SEM (n = 50). * $p < 0.05$ indicates

comparison with the control group and # $p < 0.05$ indicates comparison with the D-gal group. CM denotes coconut milk (2.5 ml/g diet); D-gal represents D-galactose (25 mg/g diet).

3.5 GC-MS analysis result

There were nineteen (19) phytoconstituents identified in the GC-MS analysis of CM. (Table 1).

Table 1: Phytoconstituents in GC-MS analysis of CM.

S/N	Compound name	RT	% of Total
1	Octanoic acid,	5.954	6.34
2	2H-Pyran-2-one, tetrahydro-6-propyl-,	7.247	1.05
3	1-Pyrrolidinecarboxaldehyde,	7.247	1.05
4	Hexanoic acid, 1,1-dimethylpropyl ester	7.247	1.05
5	n-Decanoic acid	8.180	3.84
6	2H-Pyran-2-one, tetrahydro-6-pentyl-	9.542	2.13
7	Dodecanoic acid	10.245	32.80
8	Undecanoic acid, ethyl ester,	10.314	2.93
9	delta.-Dodecalactone,	11.590	1.00
10	2H-Pyran-2-one, tetrahydro-6-octyl	11.590	1.00
11	Tetradecanoic acid	12.048	18.03
12	n-Hexadecanoic acid,	12.168	1.04
13	Heptadecane, 2-methyl-	12.168	1.04
14	Tridecanoic acid	13.719	12.70
15	11-Octadecenoic acid, methyl ester,	14.714	1.47

16	6-Octadecenoic acid, methyl ester, (Z)-,	14.714	1.47
17	trans-13-Octadecenoic acid, methyl ester	14.714	1.47
18	Oleic Acid	15.103	10.50
19	Octadecanoic acid	15.264	2.38

3.6 *In silico* result

3.6.1 Molecular docking

Table 2: Binding affinities of standards and selected phytoconstituents of CM against *D. melanogaster* AChE and GST-2 from molecular docking using the PyRx Virtual Screening tool.

S/N	Name of Compounds	PubChem CID	Binding Affinity (Kcal/mol)	
			AChE	GST-2
i.	9-(3-iodobenzylamino)-1,2,3,4-tetrahydroacridine (co-crystalized ligand) (ACHE inhibitor) – Standard I	448167	-12.0	---
ii.	Methyldopa (GST-2 activator) – Standard II	38853	---	-5.4
1	Oleic Acid	445639	-7.7	-5.1
2	Octadecanoic acid	5281	-7.5	-4.7
3	Tetradecanoic acid	11005	-7.3	-5.0
4	Tridecanoic acid	12530	-7.1	-3.8
5	Dodecanoic acid	3893	-7.0	-4.1
6	n-Decanoic acid	2969	-6.6	-4.2
7	Octanoic acid	379	-5.9	-4.0

3.6.2 Protein-ligand complex visualization

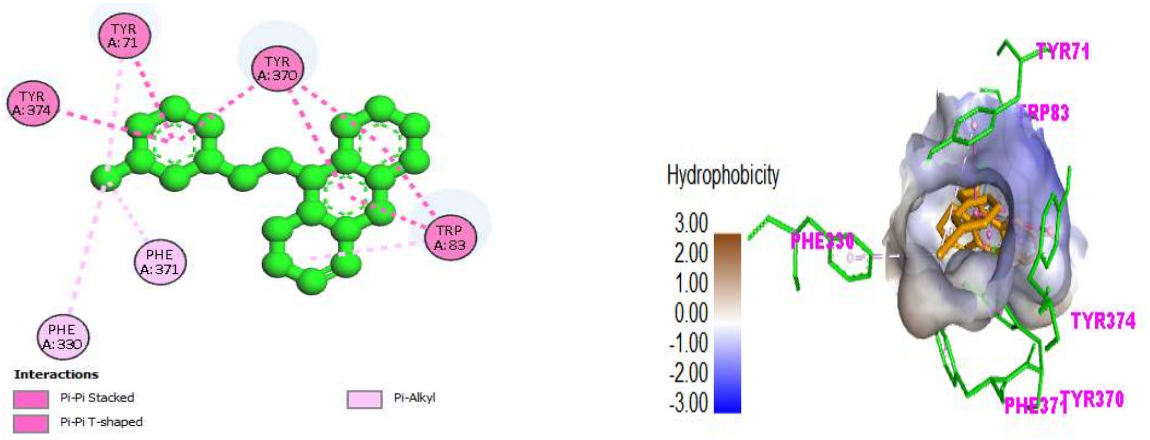

a b

FIGURE 5.1: 2D (a) and 3D (b) Interaction of *D. melanogaster AChE* and co-crystalized ligand (inhibitor) using Discovery Studio 2025.

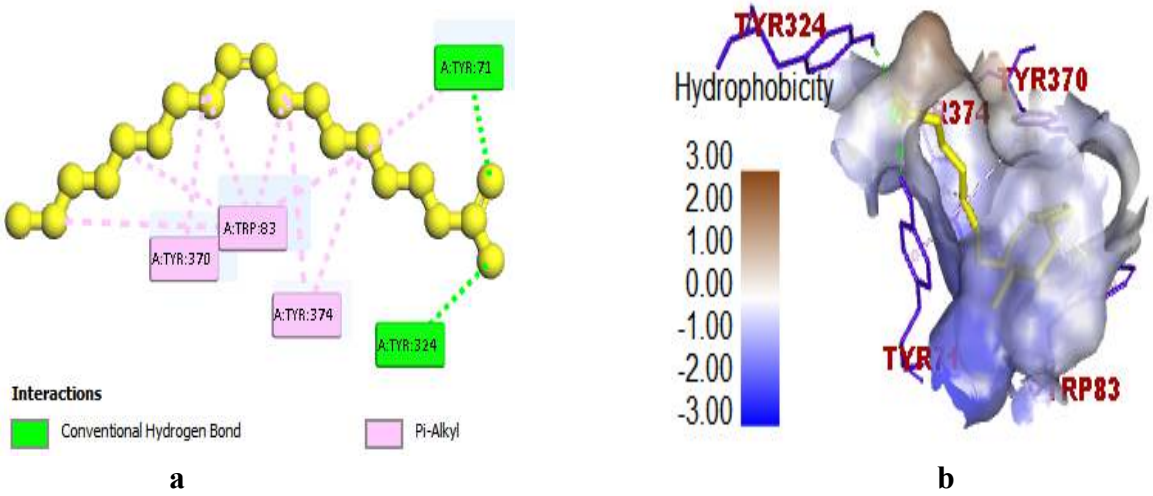

a **b**

FIGURE 5.2: 2D (a) and 3D (b) Interaction of *D. melanogaster AChE* and Oleic Acid using Discovery Studio 2025.

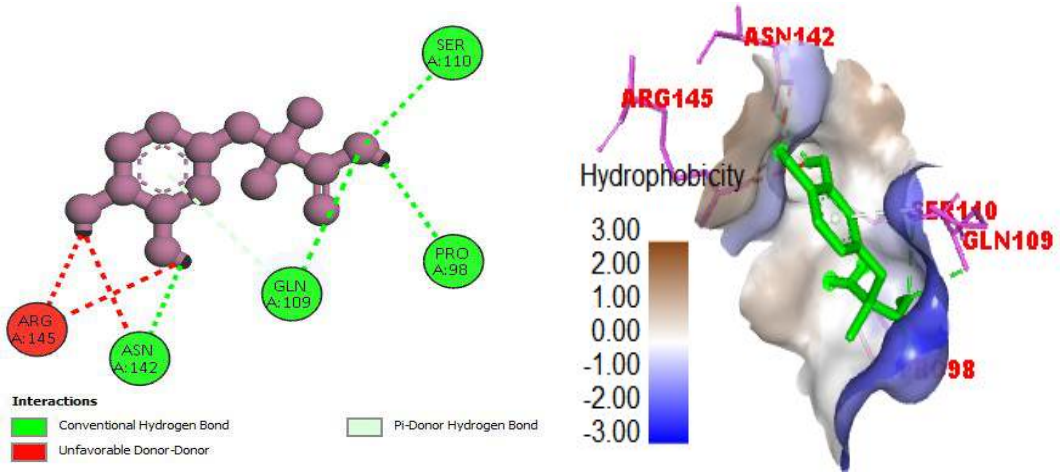

a **b**

FIGURE 5.3: 2D (a) and 3D (b) Interaction of *D. melanogaster* GST-2 and methyldopa (activator) using Discovery Studio 2025.

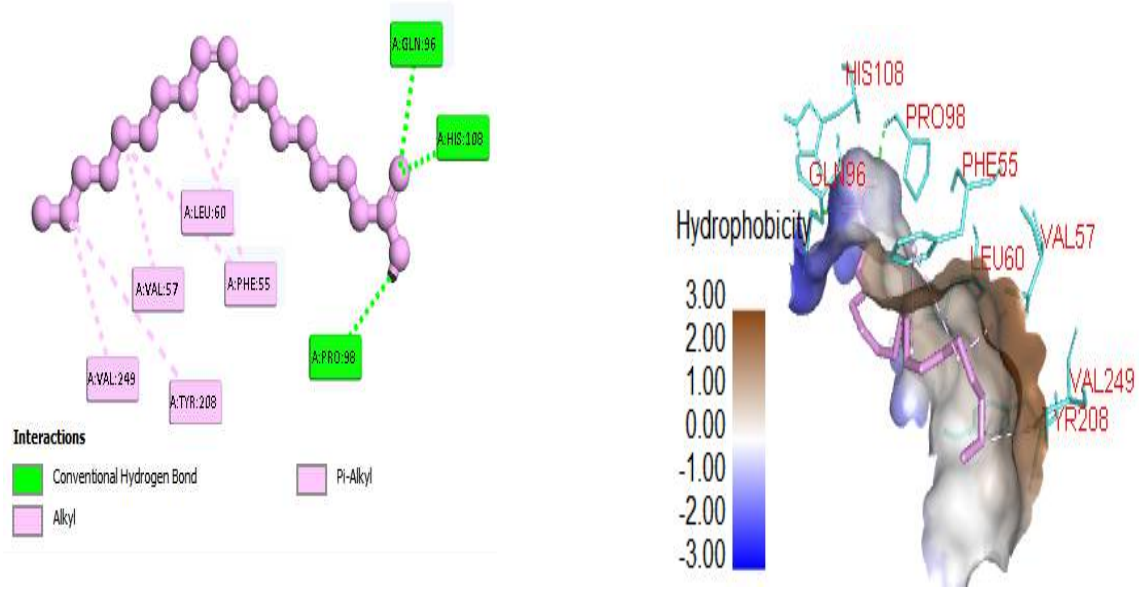

a **b**

FIGURE 5.4: 2D (a) and 3D (b) Interaction of *D. melanogaster* GST-2 and Oleic Acid using Discovery Studio 2025.

3.6.3 Interaction Tables of *D. melanogaster AChE,* GST-2, standards, and phytochemical compounds.

Table 3: Interaction Table of *D. melanogaster AChE and* co-crystalized ligand (Inhibitor).

S/N	Name	Distance	Category	Types
1	A:TYR71 - N:I40601	3.76485	Hydrophobic	Pi-Pi Stacked
2	A:TRP83 - N:I40601	3.58338	Hydrophobic	Pi-Pi Stacked
3	A:TRP83 - N:I40601	3.88309	Hydrophobic	Pi-Pi Stacked
4	A:TRP83 - N:I40601	3.88204	Hydrophobic	Pi-Pi Stacked
5	A:TRP83 - N:I40601	5.11728	Hydrophobic	Pi-Pi Stacked
6	A:TYR370 - N:I40601	4.17045	Hydrophobic	Pi-Pi Stacked
7	A:TYR370 - N:I40601	3.57376	Hydrophobic	Pi-Pi Stacked
8	A:TYR370 - N:I40601	5.15858	Hydrophobic	Pi-Pi T-shaped
9	A:TYR374 - N:I40601	4.73932	Hydrophobic	Pi-Pi T-shaped
10	A:TYR71 - N:I40601:I	5.36115	Hydrophobic	Pi-Alkyl
11	A:TRP83 - N:I40601	5.32037	Hydrophobic	Pi-Alkyl
12	A:TRP83 - N:I40601	4.35432	Hydrophobic	Pi-Alkyl
13	A:PHE330 - N:I40601:I	5.23199	Hydrophobic	Pi-Alkyl
14	A:PHE371 - N:I40601:I	5.01894	Hydrophobic	Pi-Alkyl

Table 4: Interaction Table of *D. melanogaster AChE and* Oleic Acid

S/N	Name	Distance	Category	Types
1	A:TYR71:HH - N:UNK1:O	2.03776	Hydrogen Bond	Conventional Hydrogen Bond
2	A:TYR324:HH - N:UNK1:O	2.3948	Hydrogen Bond	Conventional Hydrogen Bond
3	A:TYR71 - N:UNK1	3.69487	Hydrophobic	Pi-Alkyl
4	A:TRP83 - N:UNK1	4.95541	Hydrophobic	Pi-Alkyl
5	A:TRP83 - N:UNK1	3.61493	Hydrophobic	Pi-Alkyl
6	A:TRP83 - N:UNK1	4.178	Hydrophobic	Pi-Alkyl
7	A:TRP83 - N:UNK1:C	5.29931	Hydrophobic	Pi-Alkyl
8	A:TRP83 - N:UNK1	4.6575	Hydrophobic	Pi-Alkyl
9	A:TRP83 - N:UNK1	4.12417	Hydrophobic	Pi-Alkyl
10	A:TYR370 - N:UNK1	5.15128	Hydrophobic	Pi-Alkyl
11	A:TYR370 - N:UNK1	3.73781	Hydrophobic	Pi-Alkyl
12	A:TYR374 - N:UNK1	4.70409	Hydrophobic	Pi-Alkyl
13	A:TYR374 - N:UNK1	4.08638	Hydrophobic	Pi-Alkyl

Table 5: Interaction Table of *D. melanogaster* GST-2 *and* Methyldopa

S/N	Name	Distance	Category	Types
1	A:GLN109:N - N:UNK1:O	2.98432	Hydrogen Bond	Conventional Hydrogen Bond
2	A:SER110:N - N:UNK1:O	3.08841	Hydrogen Bond	Conventional Hydrogen Bond
3	N:UNK1:H - A:PRO98:O	2.56824	Hydrogen Bond	Conventional Hydrogen Bond
4	N:UNK1:H - A:ASN142:OD1	2.48204	Hydrogen Bond	Conventional Hydrogen Bond
5	A:GLN109:NE2 - N:UNK1	3.91409	Hydrogen Bond	Pi-Donor Hydrogen Bond

Table 6: Interaction table of *D. melanogaster* GST-2 and Oleic acid using Discovery Studio 2025.

S/N	Name	Distance	Category	Types
1	A:GLN96:HE22 - N:UNK1:O	2.36708	Hydrogen Bond	Conventional Hydrogen Bond
2	A:HIS108:HD1 - N:UNK1:O	2.16027	Hydrogen Bond	Conventional Hydrogen Bond
3	N:UNK1:H - A:PRO98:O	2.3243	Hydrogen Bond	Conventional Hydrogen Bond
4	A:VAL57 - N:UNK1	4.34247	Hydrophobic	Alkyl
5	N:UNK1 - A:LEU60	4.72489	Hydrophobic	Alkyl
6	N:UNK1:C - A:VAL249	3.86266	Hydrophobic	Alkyl
7	A:PHE55 - N:UNK1	4.58604	Hydrophobic	Pi-Alkyl
8	A:PHE55 - N:UNK1	4.8889	Hydrophobic	Pi-Alkyl
9	A:TYR208 - N:UNK1:C	5.30519	Hydrophobic	Pi-Alkyl

4.0 Discussion

This study showed the effectiveness of CM as a nutritional supplement for delaying the aging process by repairing oxidative damage, restoring antioxidant status, and improving neurotransmitter function using D-gal-induced aging in *the D. melanogaster* model. The GC–MS analysis identified 19 CM phytochemicals. Oleic acid showed the strongest binding to *D. melanogaster* AChE and GST-2, indicating inhibition of AChE and enhanced GST-2 activity, which supports the biochemical findings.

Firstly, we observed that CM progressively increases the lifespan of the flies across the increasing concentrations. This suggests that CM possesses dose-dependent life-extending effects, which may be explained by MCTs content in CM [47]. MCTs improve the lifespan through antioxidant effects by mitigating oxidative stress, a key hallmark of neurodegeneration and aging [48]. Although the 5 ml/g group exhibited the highest median survival, the absence of a statistically significant difference between the 2.5 ml/g and 5 ml/g groups suggests that increasing CM beyond 2.5 ml/g in the fruit fly diet does not confer additional survival benefit. Thus, 2.5 ml/g was selected for subsequent behavioral and biochemical analysis as the optimal dose, and this dose ameliorated the D-gal-induced reduction in longevity when relative to the D-gal-treated flies in this study.

Negative geotaxis, a crucial behavioral marker of neuromuscular function, declines with age and in neurodegenerative disorders in *D. melanogaster* [49-50]. In this study, D-gal significantly impaired locomotor performance, consistent with its known role in inducing mitochondrial dysfunction and neuronal damage [14,51]. However, co-treatment with CM markedly improved the climbing ability, suggesting a protective effect against D-gal-induced neurotoxicity. This observed locomotion improvement may be attributed to the presence of phenolic compounds (e.g.,

caffeic acid, gallic acid, vanillic acid, syringic acid, and p-hydroxybenzoic acid) that enhance mitochondrial energy production, mitigate oxidative stress, and preserve neuronal integrity [52-54].

Aging in flies can be measured by monitoring the number of offspring produced, as well as by assessing the flies' reactions to light, smell, and taste [55]. Neurogenic alterations in the olfactory bulb and epithelium are the main cause of age-related olfactory deterioration [56]. Our study revealed that exposure of *D. melanogaster* to D-gal alone significantly induced olfactory impairment (Figure 2A). This phenotypic expression agreed with the work of Chogtu *et al*. [57] Chiroma *et al*. [58] and Li *et al*. [59] who described long-term administration of D-gal hastening the aging processes via cognitive impairment and neuronal damage, which are associated with olfactory function. Partial restoration of the olfactory function by CM in this study may be due to the presence of lauric acid (dodecanoic acid) as one of the major components. Because of its antioxidant qualities and ability to provide neurons in the brain with a non-glucogenic energy source that increases oxidative mitochondrial metabolism, lauric acid improves olfactory performance [60-61].

Fertility often decreases with aging [62], and this was also validated in our study, as shown in Figure 2B. The reduced offspring emergence in the D-gal group, contrasted to the control and CM-treated groups, confirms that D-gal also induced reproductive aging in *D. melanogaster*. However, CM partially improved fertility across all the groups, and this could also be linked to the bioactive contents in CM, which can modulate hormones related to reproduction [63]. Our result is in consonance with the research of Idowu *et al*. who narrated that CM improved egg count and offspring emergence of the Parkinsonian alpha-synuclein mutant *D. melanogaster* model [32].

An increase in the body's concentration of free radicals, which harm the structure of cellular lipids, proteins, and DNA, is indicative of cellular aging [64]. In our study, D-gal significantly elevated the oxidative stress parameters (H_2O_2, MDA, and NO) as shown in Figure 3A-C. These phenotypic manifestations concurred with the reports of Rahman *et al*. and Martinovic *et al*., who narrated that D-gal promotes free radical buildup and inhibits antioxidant enzymes [65-66]. Homolak *et al.* stated that, due to an increase in ROS generation, D-gal causes cellular senescence linked to pathological diseases that cause aging [67]. Nevertheless, CM from this study restored essential antioxidant content indices (CAT, SOD, GSH, and GST) (Figures 3D-G). CM's ability to scavenge free radicals may be explained by its high vitamin B content and ability to facilitate the absorption of fat-soluble vitamins, including A, D, E, and K [68]. Aside from their well-known role in growth, metabolism, and development, vitamins also play a significant role in antioxidant defense [69]. The antioxidant effects of CM may partly involve preservation of glutathione homeostasis and modulation of oxidative stress pathways [70]. Additionally, unlike other nuts, CM also contains medium-chain saturated fatty acids (MCFAs), which reduce oxidative stress and contribute to cognition-enhancing effects and neuroprotection [71]. CM is a potential food element that prevents oxidative damage and decreases the risk of degenerative disorders [28].

Numerous biochemical alterations in the brain occur with aging [72]. Acetylcholine is essential for functions related to memory, attention, and learning. Cholinergic function declines with age, and these declines have been linked to cognitive deficits like AD [73]. Also, age-related neurological symptoms, including increased rigidity and decreased arm swing, are caused by a dopamine deficit [74]. In this present study, evidence suggests that D-gal upregulated AChE activity, reduced ACh content, and decreased dopamine level significantly in contrast to the control flies. This report is in line with the studies of Chiroma *et al*. and Salama *et al*. [58,75] who narrated

that D-gal, through the upregulation of NF-kB, initiates neuroinflammation, a key factor in brain aging. However, the MCFAs found in CM convert into ketone bodies in the liver and are then carried into the brain via monocarboxylic acid transporters [76] may be the reason for CM's ameliorative potential against these neurotransmitter defects in the CM co-treated group. Because, by boosting mitochondrial activity, decreasing oxidative damage, altering epigenetic proteins post-translationally, lowering neuroinflammation, and influencing neurotransmission systems, ketone bodies demonstrate anti-aging and neuroprotective benefits [77].

In this study, the selected phytoconstituents were docked against the active sites of *D. melanogaster* AChE and GST-2. The results demonstrated that one of the phytochemical compounds, oleic acid, have the highest binding affinity when docked with both AChE and GST-2. Oleic acid displayed a binding affinity of −7.7 kcal/mol, whereas the co-crystallized ligand (standard) resulted in a binding affinity of −12.0 kcal/mol (Table 2) when docked into the binding site of AChE. The binding interactions of oleic acid within the active site of AChE involved two hydrogen bonds and eleven hydrophobic interactions. The hydrogen bonds were formed with TYR71 and TYR324 residues, while the hydrophobic interactions involved TYR71, TRP83, TYR370, and TYR374 residues (Table 4, Figure 5.2). In contrast, the co-crystallized ligand (standard) exhibited fourteen hydrophobic interactions exclusively, involving TYR71, TRP83, TYR370, TYR374, PHE330, and PHE371 residues (Table 3, Figure 5.1). These interaction patterns suggest that oleic acid employs a similar inhibitory mechanism to that of the standard compound. Although the standard compound demonstrated a higher binding affinity than oleic acid, it did not form any hydrogen bonds, unlike oleic acid. Previous studies have reported that protein–ligand interactions are significantly facilitated by hydrogen bonding [78]. Furthermore, intermolecular hydrogen bonds have been shown to restrict internal movement within the binding

site and enhance structural stability [79]. Therefore, the binding score (−7.7 kcal/mol) observed for oleic acid indicates its inhibitory potential against *D. melanogaster* AChE. This observation is consistent with our in vivo findings and is further supported by the report of Idowu *et al*., who demonstrated a significant decrease ($p < 0.01$, $p < 0.001$) in AChE activity in CM-treated *D. melanogaster* compared to the untreated group [32]. Similarly, Casertano *et al*. reported that elevated levels of NO, MDA, and AChE were reduced by CM administration at all tested concentrations, which may be attributed to the neuromodulatory properties of CM [80].

With respect to GST-2, oleic acid showed a binding affinity of −5.1 kcal/mol, while methyldopa (the standard compound) showed a slightly higher binding affinity of −5.4 kcal/mol (Table 2). However, oleic acid utilized both hydrogen bonding and hydrophobic interactions to bind to the active site of GST-2, whereas methyldopa relied solely on hydrogen bonding. Specifically, the binding interactions of oleic acid within the GST-2 active site comprised three (3) hydrogen bonds and six (6) hydrophobic interactions. The hydrogen bonds involved GLN96, HIS108, and PRO98 residues, while the hydrophobic interactions involved VAL57, LEU60, VAL249, PHE55, and TYR208 residues (Table 6, Figure 5.4). In comparison, methyldopa formed five (5) hydrogen bonds involving GLN109, SER110, PRO98, and ASN142 residues (Table 5, Figure 5.3). The interaction profile of oleic acid observed in this study highlights its antioxidant potential. This finding is supported by our in vivo experiments and represents the first report demonstrating that CM enhances the antioxidant activity of GST-2 in *D. melanogaster*.

5.0 Conclusion

This study provides evidence that CM has anti-aging and neuroprotective effects against D-gal-induced toxicity in *D. melanogaster*. CM supplementation in the diet significantly enhanced the life span, locomotor performance, and olfactory response while partially attenuated the fecundity and restored the redox homeostasis and neurotransmitter balance disrupted by D-gal exposure. Biochemical results indicate that the mechanisms of CM against oxidative stress involve the enhancement of endogenous antioxidant indices (SOD, CAT, GSH, and GST) and suppression of lipid peroxidation and nitric oxide levels. Furthermore, molecular docking results support the neuromodulatory and antioxidative potential of major bioactive constituents of CM due to their strong binding affinities for AChE and GST-2. This suggests that CM is a functional food that may have potential in mitigating age-related neurodegenerative and oxidative impairments, probably because of its rich composition of MCFAs, vitamins, and polyphenolic bioactive compounds.

Despite the promising result of this study, certain limitations need to be acknowledged. While behavioral and biochemical biomarkers related to aging and neurodegeneration were assessed, further studies are needed on the effect of CM on dopaminergic neuron loss, inflammatory biomarkers, protein aggregation, and gene expression analysis of age and neurodegeneration related pathways. Furthermore, validating these findings in mammalian models is also necessary, as the results with the *D. melanogaster* model might not fully recapitulate the complexity of mammalian systems.

Hightlighs

- Coconut milk attenuated D-gal-induced aging and neurotoxicity in *Drosophila.*
- Coconut milk improved antioxidant defenses and restored locomotor behavior.
- Coconut phytochemicals showed strong binding affinity to AChE and GST-2.

CRediT authorship contribution statement

Arogundade Muideen Tunde: Writing: data curation, conceptualization, visualization, validation, formal analysis, methodology, investigation, and original draft. **Raji Rafiu Adekunle:** Writing: data curation, validation, visualization, methodology, formal analysis, investigation, and original draft. **Jimoh Kamiludeen Ayinla**: Writing: investigation, data curation, validation, methodology, visualization, and formal analysis. **Atere Tope Gafar**: Supervision, editing & review.

Disclosure of competing interests

The authors did not disclose any possible conflicts of interest.

Funding

None

Data availability

On reasonable request from the corresponding author, data will be made available upon request.

Ethics Approval

Not applicable

References

1. M. E. Rusu, I. Fizeșan, L. Vlase and D. S. Popa, Antioxidants in age-related diseases and anti-aging strategies, *Antioxidants*, 2022, **11**, 1868.

2. I. S. Pyo, S. Yun, Y. E. Yoon, J. W. Choi and S. J. Lee, Mechanisms of aging and the preventive effects of resveratrol on age-related diseases, *Molecules*, 2020, **25**, 4649.

3. J. Guo, X. Huang, L. Dou, M. Yan, T. Shen, W. Tang and J. Li, Aging and aging-related diseases: from molecular mechanisms to interventions and treatments, *Signal Transduct. Target. Ther.*, 2022, **7**, 391.

4. P. Li, Y. Ma, X. Wang, X. Li, X. Wang, J. Yang and G. Liu, The protective effect of PL1-3 on D-galactose-induced aging mice, *Front. Pharmacol.*, 2024, **14**, 1304801.

5. P. Sobhon, G. Savedvanich and S. Weerakiet, Oxidative stress and inflammation: the root causes of aging, *Explor. Med.*, 2023, **4**, 127–156.

6. S. Azam, M. E. Haque, R. Balakrishnan, I. S. Kim and D. K. Choi, The ageing brain: molecular and cellular basis of neurodegeneration, *Front. Cell Dev. Biol.*, 2021, **9**, 683459.

7. J. E. Palmer, N. Wilson, S. M. Son, P. Obrocki, L. Wrobel, M. Rob *et al.*, Autophagy, aging, and age-related neurodegeneration, *Neuron*, 2025, **113**, 29–48.

8. H. J. Lee, Y. S. Yoon and S. J. Lee, Molecular mechanisms of cellular senescence in neurodegenerative diseases, *J. Mol. Biol.*, 2023, **435**, 168114.

9. T. Shwe, W. Pratchayasakul, N. Chattipakorn and S. C. Chattipakorn, Role of D-galactose-induced brain aging and its potential use for therapeutic interventions, *Exp. Gerontol.*, 2018, **101**, 13–36.

10. A. Hosseini, L. Ziaee, A. Rajabian and M. T. Boroushaki, Protective effect of pomegranate seed oil against D-galactose-induced aging in rats, *J. Adv. Med. Biomed. Res.*, 2023, **31**, 80–85.

11. M. Celina, E. Linde, D. Brunson, A. Quintana and N. Giron, Overview of accelerated aging and polymer degradation kinetics for combined radiation-thermal environments, *Polym. Degrad. Stab.*, 2019, **166**, 353–378.

12. K. F. Azman and R. Zakaria, D-Galactose-induced accelerated aging model: an overview, *Biogerontology*, 2019, **20**, 763–782.

13. H. Kumar, K. Bhardwaj, M. Valko, S. Y. Alomar, S. H. Alwasel, N. Cruz-Martins *et al.*, Antioxidative potential of *Lactobacillus* sp. in ameliorating D-galactose-induced aging, *Appl. Microbiol. Biotechnol.*, 2022, **106**, 4831–4843.

14. O. T. Oyebode, A. O. Abolaji, J. O. Oluwadare, A. O. Adedara and O. O. Olorunsogo, Apigenin ameliorates D-galactose-induced lifespan shortening effects via antioxidative activity and inhibition of mitochondrial-dependent apoptosis in *Drosophila melanogaster*, *J. Funct. Foods*, 2020, **69**, 103957.

15. O. Mahdi, S. M. Chiroma, M. T. H. Baharuldin, N. H. Mohd Nor, C. N. Mat Taib, S. Jagadeesan *et al.*, Win55,212-2 attenuates cognitive impairments in $AlCl_3$ + D-galactose-induced Alzheimer's disease rats by enhancing neurogenesis and reversing oxidative stress, *Biomedicines*, 2021, **9**, 1270.

16. B. S. Alotaibi, U. Saleem, M. Farrukh, S. Waseem, Z. Chauhdary, I. Alsharif *et al.*, Chamuangone-rich rice bran oil ameliorates neurodegeneration in $AlCl_3$/D-galactose model via modulation of behavioral, biochemical and neurochemical parameters, *Ital. J. Food Sci.*, 2024, **36**.

17. S. Saiyasilp, S. Vaseenon, T. Srisuwan and P. Chuveera, Effects of D-galactose induction on aging characteristics of the human dental pulp cell culture model: an in vitro study, *Eur. Endod. J.*, 2025, **10**, 142–150.

18. R. S. Rosen and M. L. Yarmush, Current trends in anti-aging strategies, *Annu. Rev. Biomed. Eng.*, 2023, **25**, 363–385.

19. A. Hruby, S. Sahni, D. Bolster and P. F. Jacques, Protein intake and functional integrity in aging: the Framingham heart study offspring, *J. Gerontol. Ser. A*, 2020, **75**, 123–130.

20. M. Kuzuya, Nutritional status related to poor health outcomes in older people: which is better, obese or lean?, *Geriatr. Gerontol. Int.*, 2021, **21**, 5–13.

21. B. F. Kocyigit, E. Kocyigit and G. Y. Ozturk, Anti-aging nutrition therapy, *Anti-Aging East. Eur.*, 2024, **3**, 59–65.

22. J. H. Cole, R. E. Marioni, S. E. Harris and I. J. Deary, Brain age and other bodily 'ages': implications for neuropsychiatry, *Mol. Psychiatry*, 2019, **24**, 266–281.

23. M. Fekete, Z. Szarvas, V. Fazekas-Pongor, A. Feher, T. Csipo, J. Forrai *et al.*, Nutrition strategies promoting healthy aging: from improvement of cardiovascular and brain health to prevention of age-associated diseases, *Nutrients*, 2022, **15**, 47.

24. H. M. Henrietta, K. Kalaiyarasi and A. S. Raj, Coconut tree (*Cocos nucifera*) products: a review of global cultivation and its benefits, *J. Sustain. Environ. Manage.*, 2022, **1**, 257–264.

25. W. Liu, The nutritional elixir: unveiling the benefits of coconut milk, *J. Nutr. Food Sci.*, 2023, **13**, 060.

26. H. Ishikawa, K. Kojima, S. Watanabe, N. Nosaka and T. Mutoh, Effect of medium-chain triglyceride supplements and walking on health-related quality of life in sedentary, healthy middle-aged and older adults with low BMIs: a randomized, double-blind, placebo-controlled, parallel-group trial, *Front. Nutr.*, 2023, **10**, 1296896.

27. G. L. Russo, C. Spagnuolo, M. Russo, I. Tedesco, S. Moccia and C. Cervellera, Mechanisms of aging and potential role of selected polyphenols in extending healthspan, *Biochem. Pharmacol.*, 2020, **173**, 113719.

28. S. Alyaqoubi, A. Abdullah, M. Samudi, N. Abdullah, Z. R. Addai and K. H. Musa, Study of antioxidant activity and physicochemical properties of coconut milk (*Pati santan*) in Malaysia, *J. Chem. Pharm. Res.*, 2015, **7**, 967–973.

29. K. Darsana, O. Bashir, S. Morya, P. A. Pawase, I. H. Mondal, T. Amin and R. Mugabi, Coconut milk as a plant-based dairy alternative: developmental trends and assessing carbon footprint impact, *Discover Food*, 2026, **6**, 25.

30. A. A. Ogienko, E. S. Omelina, O. V. Bylino, M. A. Batin, P. G. Georgiev and A. V. Pindyurin, *Drosophila* as a model organism to study basic mechanisms of longevity, *Int. J. Mol. Sci.*, 2022, **23**, 11244.

31. M. D. Piper and L. Partridge, *Drosophila* as a model for ageing, *Biochim. Biophys. Acta Mol. Basis Dis.*, 2018, **1864**, 2707–2717.

32. O. Idowu, O. Dosumu and A. Oremosu, Coconut milk ameliorates motor and non-motor deficits in the alpha-synuclein transgenic *Drosophila melanogaster* model for Parkinsonism, *Sule Lamido Univ. J. Sci. Technol.*, 2022, **5**, 62–72.

33. T. G. Atere, M. T. Arogundade, O. O. Adewale and O. K. Idowu, Therapeutic potential of *Ocimum gratissimum* biogenic ZnO-nanoparticles on rotenone-induced neurotoxicity in *Drosophila melanogaster*, *BioNanoScience*, 2025, **15**, 339.

34. E. O. Farombi, A. O. Abolaji, T. H. Farombi, A. S. Oropo, O. A. Owoje and M. T. Awunah, *Garcinia kola* seed biflavonoid fraction (Kolaviron) increases longevity and attenuates rotenone-induced toxicity in *Drosophila melanogaster*, *Pestic. Biochem. Physiol.*, 2018, **145**, 39–45.

35. T. T. Men, D. T. Khang, N. T. Tuan and D. T. X. Trang, Anti-aging effects of *Lasia spinosa* L. stem extract on *Drosophila melanogaster*, *Food Sci. Technol.*, 2021, **42**, e38721.

36. T. G. Atere, D. K. Wahyuni, O. J. Avwioroko, A. A. Bayo-Olugbami, O. K. Idowu, M. T. Arogundade *et al.*, Proanthocyanidin from grape seed against rotenone-induced toxicity in *Drosophila melanogaster*: insights from behavioural and antioxidant studies, *Not. Sci. Biol.*, 2025, **17**, 12341.

37. L. L. Vang, A. V. Medvedev and J. Adler, Simple ways to measure behavioral responses of *Drosophila* to stimuli and use of these methods to characterize a novel mutant, *PLoS One*, 2012, **7**, e37495.

38. O. K. Idowu, A. A. Oremosu, O. O. Dosumu and A. A. Mohammed, Ribose-cysteine and levodopa abrogate Parkinsonism via the regulation of neurochemical and redox activities in alpha-synuclein transgenic *Drosophila melanogaster* models, *Fly*, 2024, **18**, 2306687.

39. O. M. Ighodaro and O. A. Akinloye, First line defence antioxidants-superoxide dismutase (SOD), catalase (CAT) and glutathione peroxidase (GPX): their fundamental role in the entire antioxidant defence grid, *Alex. J. Med.*, 2018, **54**, 287–293.

40. W. H. Habig and W. B. Jakoby, Assays for differentiation of glutathione S-transferases, *Methods Enzymol.*, 1981, **77**, 398–405.

41. M. Sun and S. Zigman, An improved spectrophotometric assay for superoxide dismutase based on epinephrine autoxidation, *Anal. Biochem.*, 1978, **90**, 81–89.

42. J. Sedlak and R. H. Lindsay, Estimation of total, protein-bound and nonprotein sulfhydryl groups in tissue with Ellman's reagent, *Anal. Biochem.*, 1968, **25**, 192–205.

43. S. G. Rhee and H. A. Woo, Multiple functions of peroxiredoxins: peroxidases, sensors and regulators of the intracellular messenger H_2O_2, and protein chaperones, *Antioxid. Redox Signaling*, 2011, **15**, 781–794.

44. I. Eleftherianos, K. More, S. Spivack, E. Paulin, A. Khojandi and S. Shukla, Nitric oxide levels regulate the immune response of *Drosophila melanogaster* reference laboratory strains to bacterial infections, *Infect. Immun.*, 2014, **82**, 4169–4181.

45. F. Karatas, M. Karatepe and A. Baysar, Determination of free malondialdehyde in human serum by high-performance liquid chromatography, *Anal. Biochem.*, 2002, **311**, 76–79.

46. G. O. Ambrose, O. J. Afees, N. C. Nwamaka, N. Simon, A. A. Oluwaseun, T. Soyinka, A. S. Oluwaseun and S. Bankole, Selection of luteolin as a potential antagonist from molecular docking analysis of EGFR mutant, *Bioinformation*, 2018, **14**, 241–247.

47. L. Boemeke, A. Marcadenti, F. M. Busnello and C. B. A. Gottschall, Effects of coconut oil on human health, *Open J. Endocr. Metab. Dis.*, 2015, **5**, 84–87.

48. Y. Liu, M. Fang, X. Tu, X. Mo, L. Zhang, B. Yang *et al.*, Dietary polyphenols as anti-aging agents: targeting the hallmarks of aging, *Nutrients*, 2024, **16**, 3305.

49. J. Tower, S. Agrawal, M. P. Alagappan, H. S. Bell, M. Demeter, N. Havanoor *et al.*, Behavioral and molecular markers of death in *Drosophila melanogaster*, *Exp. Gerontol.*, 2019, **126**, 110707.

50. J. Tower, Markers and mechanisms of death in *Drosophila*, *Front. Aging*, 2023, **4**, 1292040.

51. Y. Xu, M. Xue, J. Li, Y. Ma, Y. Wang, H. Zhang and H. Liang, Fucoidan improves D-galactose-induced cognitive dysfunction by promoting mitochondrial biogenesis and maintaining gut microbiome homeostasis, *Nutrients*, 2024, **16**, 1512.

52. W. M. A. D. B. Fernando, I. J. Martins, K. G. Goozee, C. S. Brennan, V. Jayasena and R. N. Martins, The role of dietary coconut for the prevention and treatment of Alzheimer's disease: potential mechanisms of action, *Br. J. Nutr.*, 2015, **114**, 1–14.

53. A. N. Karunasiri, M. Gunawardane, C. M. Senanayake, N. Jayathilaka and K. N. Seneviratne, Antioxidant and nutritional properties of domestic and commercial coconut milk preparations, *Int. J. Food Sci.*, 2020, **2020**, 3489605.

54. M. Gunawardane, N. Jayathilaka and K. N. Seneviratne, Coconut milk phenolics enhance general oxidative-stress resistance and specifically protect against lipid peroxidation in selected bacteria, *J. Agric. Value Addit.*, 2025, **8**.

55. A. Tsurumi and W. X. Li, Aging mechanisms—A perspective mostly from *Drosophila*, *Adv. Genet.*, 2020, **1**, e10026.

56. X. Dan, N. Wechter, S. Gray, J. G. Mohanty, D. L. Croteau and V. A. Bohr, Olfactory dysfunction in aging and neurodegenerative diseases, *Ageing Res. Rev.*, 2021, **70**, 101416.

57. B. Chogtu, A. Arivazhahan, S. K. Kunder, A. Tilak, R. Sori and A. Tripathy, Evaluation of acute and chronic effects of D-galactose on memory and learning in Wistar rats, *Clin. Psychopharmacol. Neurosci.*, 2018, **16**, 153.

58. S. M. Chiroma, M. T. H. Baharuldin, C. N. M. Taib, Z. Amom, S. Jagadeesan, M. I. Adenan and M. A. M. Moklas, Protective effect of *Centella asiatica* against D-galactose and aluminium chloride-induced rats: behavioral and ultrastructural approaches, *Biomed. Pharmacother.*, 2019, **109**, 853–864.

59. M. Li, M. Zhu, W. Quan, W. Huang, X. Liu, C. Zhang *et al.*, Acteoside palliates D-galactose-induced cognitive impairment by regulating intestinal homeostasis, *Food Chem.*, 2023, **421**, 135978.

60. C. Veyrat-Durebex, P. Reynier, V. Procaccio, R. Hergesheimer, P. Corcia, C. R. Andres and H. Blasco, How can a ketogenic diet improve motor function?, *Front. Mol. Neurosci.*, 2018, **11**, 15.

61. N. S. Anuar, S. A. Shafie, M. A. F. Maznan, N. S. N. M. Zin, N. A. S. Azmi, R. A. Raoof *et al.*, Lauric acid improves hormonal profiles, antioxidant properties, sperm quality and histomorphometric changes in testis and epididymis of streptozotocin-induced diabetic infertility rats, *Toxicol. Appl. Pharmacol.*, 2023, **470**, 116558.

62. R. Lee and C. C. Chu, Theoretical perspectives on reproductive aging, *Front. Ecol. Evol.*, 2023, **10**, 934732.

63. K. L. Pang, J. N. Lumintang and K. Y. Chin, Thyroid-modulating activities of olive and its polyphenols: a systematic review, *Nutrients*, 2021, **13**, 529.

64. D. N. Ahsani and I. Fidianingsih, Age-related changes of malondialdehyde, body weight and organ weight in male mice, *Univ. Med.*, 2018, **37**, 115–126.

65. M. A. Rahman, A. A. Shuvo, A. K. Bepari, M. Hasan Apu, M. C. Shill, M. Hossain *et al.*, Curcumin improves D-galactose and normal-aging associated memory impairment in mice: in vivo and in silico-based studies, *PLoS One*, 2022, **17**, e0270123.

66 J. Martinovic, I. Gusevac Stojanovic, S. Nesic, A. Todorovic, K. Bobic, S. Stankovic and D. Drakulic, Chronic oral D-galactose induces oxidative stress but not overt organ dysfunction in male Wistar rats, *Curr. Issues Mol. Biol.*, 2025, **47**, 161.

67. J. Homolak, A. Babic Perhoc, D. Virag, A. Knezovic, J. Osmanovic Barilar and M. Salkovic-Petrisic, D-galactose might mediate some of the skeletal muscle hypertrophy-promoting effects of milk—A nutrient to consider for sarcopenia?, *BioEssays*, 2024, **46**, 2300061.

68. S. K. Tulashie, J. Amenakpor, S. Atisey, R. Odai and E. E. A. Akpari, Production of coconut milk: a sustainable alternative plant-based milk, *Case Stud. Chem. Environ. Eng.*, 2022, **6**, 100206.

69. O. O. Sinbad, A. A. Folorunsho, O. L. Olabisi, O. A. Ayoola and E. J. Temitope, Vitamins as antioxidants, *J. Food Sci. Nutr. Res.*, 2019, **2**, 214–235.

70. E. E. van de Lagemaat, L. C. de Groot and E. G. van den Heuvel, Vitamin B12 in relation to oxidative stress: a systematic review, *Nutrients*, 2019, **11**, 482.

71. J. Mett and U. Müller, The medium-chain fatty acid decanoic acid reduces oxidative stress levels in neuroblastoma cells, *Sci. Rep.*, 2021, **11**, 6135.

72. J. Lee and H. J. Kim, Normal aging induces changes in the brain and neurodegeneration progress: review of the structural, biochemical, metabolic, cellular and molecular changes, *Front. Aging Neurosci.*, 2022, **14**, 931536.

73. W. Lothar, Cellular and molecular basis of neurodegenerative diseases: unraveling the pathological cascade, *Integr. Neuro. Res.*, 2023, **6**, 149.

74. V. Nikhra, The aging brain: recent research and concepts, *Gerontol. Geriatr. Stud.*, 2017, **1**, 1–11.

75. A. Salama and Z. A. E. El Shahed, Naringin attenuates D-galactose-induced brain aging via regulation of oxidative stress markers TNF-α, NF-κβ and modulation of the neurotrophic markers PGC1-α, NT-3, AGEs and GFAP in vivo, *Egypt. J. Chem.*, 2024, **67**, 1–15.

76. J. John, N. K. Sapa and R. R. Shenoy, Virgin coconut oil ameliorates colchicine-induced cognitive dysfunction: a preclinical study, *Pharm. Sci.*, 2020, **26**, 1–12.

77. J. Jang, S. R. Kim, J. E. Lee, S. Lee, H. J. Son, W. Choe *et al.*, Molecular mechanisms of neuroprotection by ketone bodies and ketogenic diet in cerebral ischemia and neurodegenerative diseases, *Int. J. Mol. Sci.*, 2023, **25**, 124.

78. S. Salentin, V. J. Haupt, S. Daminelli and M. Schroeder, Polypharmacology rescored: protein–ligand interaction profiles for remote binding site similarity assessment, *Prog. Biophys. Mol. Biol.*, 2014, **116**, 174–186.

79. R. Singh, V. K. Bhardwaj, P. Das and R. Purohit, A computational approach for rational discovery of inhibitors for non-structural protein 1 of SARS-CoV-2, *Comput. Biol. Med.*, 2021, **135**, 104555.

80. M. Casertano, V. Fogliano and D. Ercolini, Psychobiotics, gut microbiota and fermented foods can help preserving mental health, *Food Res. Int.*, 2022, **152**, 110892.

Supplementary Files

This is a list of supplementary files associated with this preprint. Click to download.

- floatimage1.jpeg